Manuscript title:

Covering soybean leaves with cellulose nanofiber changes leaf surface hydrophobicity and confers resistance against *Phakopsora pachyrhizi*

Authors' full names:

Haruka Saito[1], Yuji Yamashita[1], Nanami Sakata[1], Takako Ishiga[1], Nanami Shiraishi[1], Viet Tru Nguyen[2], Eiji Yamamura[1] and Yasuhiro Ishiga[1*]

Institution addresses:

[1]Faculty of Life and Environmental Sciences, University of Tsukuba, 1-1-1 Tennodai, Tsukuba, Ibaraki 305-8572, Japan.

[2]Western Highlands Agriculture and Forestry Science Institute, Nguyen Luong Bang, Buon Ma Thuot, Dak Lak, Vietnam.

*For correspondence:

Yasuhiro Ishiga

Address: Faculty of Life and Environmental Sciences, University of Tsukuba, 1-1-1 Tennodai, Tsukuba, Ibaraki 305-8572, Japan.

Email: ishiga.yasuhiro.km@u.tsukuba.ac.jp

Tel/Fax (+81) 029-853-4792

Abstract

Asian soybean rust (ASR) caused by *Phakopsora pachyrhizi*, an obligate biotrophic fungal pathogen, is the most devastating soybean production disease worldwide. Currently, timely fungicide application is the only means to control ASR in the field. We investigated cellulose nanofiber (CNF) application on ASR disease management. CNF-treated leaves showed reduced lesion number after *P. pachyrhizi* inoculation compared to control leaves, indicating that covering soybean leaves with CNF confers *P. pachyrhizi* resistance. We also demonstrated that formation of *P. pachyrhizi* pre-infection structures including germ-tubes and appressoria, and also gene expression related to these formations, such as *chitin synthases* (*CHSs*), were significantly suppressed in CNF-treated soybean leaves compared to control leaves. Moreover, contact angle measurement revealed that CNF converts soybean leaf surface properties from hydrophobic to hydrophilic. These results suggest that CNF can change soybean leaf surface hydrophobicity, conferring resistance against *P. pachyrhizi*, based on the reduced expression of *CHSs*, as well as reduced formation of pre-infection structures. This is the first study to investigate CNF application to control field disease.

Keywords

Asian soybean rust; Cellulose nanofiber; *Chitin synthase*; Hydrophobicity; *Phakopsora pachyrhizi*; Pre-infection structure

Introduction

Diseases in important crop plants have a significant negative impact on agricultural productivity. For example, Asian soybean rust (ASR) caused by *Phakopsora pachyrhizi*, an obligate biotrophic fungal pathogen, is the most devastating soybean production disease worldwide, with an estimated crop yield loss of up to 90%. ASR has impacted the South American economy in recent years. Yorinori et al. (1) reported that the losses caused by ASR were ~2 billion US dollars in Brazil alone in 2003. Although most rust fungi have a high host specificity, the *P. pachyrhizi* host range is broad and can infect diverse leguminous plant leaves in the field (2). The infection process starts when urediniospores germinate to produce a single germ-tube with an appressorium. Unlike cereal rust fungi that penetrates through stomata (3), *P. pachyrhizi* directly penetrates into host plant epidermal cells by an appressorial peg. After penetration, *P. pachyrhizi* extends the infection hyphae and forms haustoria (feeding structures) in the mesophyll cells 24 to 48 hours after infection (4). At five to eight days after infection, *P. pachyrhizi* then produces urediniospores by asexual reproduction (4). Urediniospores can be dispersed by wind and germinate on other host plants.

There are several ASR control methods for soybean protection against *P. pachyrhizi*, including chemical control by fungicide application, growing ASR resistant soybean cultivars, and employing cultivation practices. Synthetic fungicides are the primary ASR disease control method. However, fungicide use can cause many problems such as environmental impacts (5), increased production costs (6), and the emergence of fungicide-resistant pathogens (7, 8). Another major and effective control method is breeding or engineering of ASR resistant soybean cultivars. Analysis of soybean accessions disclosed six dominant *R* genes conferring resistance to a particular *P. pachyrhizi* race, and these loci were referred to as the *Rpp* 1–6 genes (9–13). However,

none of the soybean accessions in the world show resistance to all *P. pachyrhizi* races (14). Due to the limited resistance available in soybean cultivars, heterologous expression of resistance genes from other plant species in soybean has been investigated as an alternative source of ASR resistance. Kawashima et al. (15) reported that soybean plants expressing *CcRpp1* (*Cajanus cajan* Resistance against *Phakopsora pachyrhizi 1*) from pigeon pea (*Cajanus cajan*) showed full resistance against *P. pachyrhizi*. Conversely, identifying resistance traits from non-host plant species has become an intelligent approach. Uppalapati et al. (16) screened *Medicago truncatula Tnt1* mutant lines and identified an *inhibitor of rust germ tube differentiation 1* (*irg1*) mutant with reduced formation of pre-infection structures, including germ-tubes and appressoria. They demonstrated that the loss of abaxial epicuticular wax accumulation resulting in reduced surface hydrophobicity inhibited formation of pre-infection structures on the *irg1* mutant (16). Furthermore, Ishiga et al. (17) reported that gene expression related to pre-infection structure formation were activated on the hydrophobic surface of the *M. truncatula* wild-type, but not on the *irg1* mutant, based on *P. pachyrhizi* transcriptome analysis, suggesting that leaf surface hydrophobicity can trigger gene expression related to formation of pre-infection structures. Based on these previous studies, we hypothesized that modification of leaf surface hydrophobicity might be a useful strategy to conferring resistance against *P. pachyrhizi*.

Cellulose is an organic polysaccharide consisting of a β-1,4 linked glucopyranose skeleton. Cellulose is an important structural component of plant primary cell walls and is essential in maintaining the plant structural phase. Due to the positive properties, cellulose has been investigated as an application in different research and development fields including energy, environmental, water, and biomedical related fields (18). Cellulose nanofiber (CNF), which can be derived from cellulose, is one of

the most abundant and renewable biomasses in nature (19). Because CNF exhibits properties such as low weight, high aspect ratio, high strength, high stiffness, and large surface area, CNF potentially has wide areas of application. There are several CNF isolation methods, e.g. acid hydrolysis, enzymatic hydrolysis, and mechanical processes. The aqueous counter collision (ACC) method can make it possible to cleave interfacial interactions among cellulose molecules without any chemical modification (20). Both hydrophobic and hydrophilic sites co-exist in a cellulose molecule resulting in amphiphilic properties when CNF is derived from the ACC method. Kose et al. (21) reported that coating with CNF derived from the ACC method could switch surface hydrophilic and hydrophobic properties, depending on substrate characteristics. They demonstrated that coating a filter paper and polyethylene with CNF changed the surface property into hydrophobic and hydrophilic, respectively (21). To investigate the potential application of CNF in agriculture, we examined whether coating with CNF protected soybean plants against *P. pachyrhizi*. We show that a specific CNF property can change soybean leaf surface hydrophobicity, resulting in reduced formation of pre-infection structures associated with reduced *P. pachyrhizi* infection.

Materials & Methods

Plant growth conditions, CNF treatment and pathogen inoculation assay

Susceptible soybean cultivar seeds (*Glycine max* cv. Enrei) were germinated in a growth chamber at 25°C/20°C with 16-hrs-light/8-hrs-dark cycle (100-150 μ mol m^{-2} s^{-1}) for 3 to 4 weeks.

Cellulose nanofiber (CNF, marketed as nanoforest®) supplied through the courtesy of the Chuetsu Pulp & Paper (Takaoka, Japan) was used. A bamboo-derived CNF (BC) and a needle-leaved tree-derived CNF (NC) were adjusted to a concentration

of 0.1% including 0.02% Tween 20 (FUJIFILM, Tokyo, Japan) before treatment. Both adaxial and abaxial sides of soybean leaves were spray-treated with 0.1% CNF till runoff and then the treated soybean plants were dried at room temperature for 3 to 4 hours before inoculation.

An isolate of the ASR pathogen *P. pachyrhizi* T1-2 (22) was maintained on soybean leaves. Fresh urediniospores were collected and suspended in distilled water with 0.001% Tween 20. The 3-week-old soybean plants were spray-inoculated with 1 x 10^5 spores/ml using a hand sprayer for uniform spore deposition. The inoculated plants were maintained in a chamber for 24 hours with 90% to 95% humidity at 23°C; 0-hrs-light/24-hrs-dark cycle. The plants were then transferred to a growth chamber (22°C/20 °C with 16 hrs-light/8 hrs-dark cycle) and incubated further to allow symptom development.

To quantify lesion number on ASR on CNF-treated plants, soybean leaves were spray-inoculated with *P. pachyrhizi*. At 10 days after inoculation, photographs were taken, and lesions were counted to calculate the lesion number per cm^2. Lesions were counted from 54 random fields on three independent leaves.

To quantify the formation of pre-infection structures including germ-tubes and appressoria on control and CNF-treated plants, soybean leaves were spray-inoculated with *P. pachyrhizi* 1 x 10^5 spores/ml. At 72 hours after inoculation, the leaves were observed and photographed with the desktop scanning electron microscope (HITACHI TM3000, Tokyo, Japan). The germ-tubes forming differentiated appressoria were counted as appressoria. The differentiated germ-tubes without appressoria that grew on the leaf surface were also counted from 54 random fields on three independent leaves.

Real-time quantitative RT-PCR analyses

To investigate the gene expression profiles related to pre-infection structures, approximately 100 *P. pachyrhizi* spores in 10 µl aliquots were placed on the abaxial surface of 4-week-old detached soybean leaves with or without 0.1% CNF and incubated in darkness overnight, and then transferred to a growth chamber (22°C/20°C with 16-h-light/8-h-dark cycle). At 24 and 48 hours after inoculation, total RNA was extracted from the inoculated leaf areas and purified using RNAiso Plus (TaKaRa, Otsu, Japan) according to the manufacture's protocol. For soybean *pathogenesis-related gene protein 1* (*GmPR1*) expression profiles, soybean leaves were treated with or without 0.1% CNF. At 24 hours after CNF treatment, total RNA was extracted from leaves and purified using RNAiso Plus (TaKaRa) according to the manufacture's protocol. Two micrograms of total RNA were treated with gDNA Remover (TOYOBO, Osaka, Japan) to eliminate genomic DNA, and the DNase-treated RNA was reverse transcribed using the ReverTra Ace qPCR RT Master Mix (TOYOBO). The cDNA (1:10) was then used for RT-qPCR using the primers shown in Supplementary Table S1 with THUNDERBIRD SYBR qPCR Mix (TOYOBO) on a Thermal Cycler Dice Real Time System (TaKaRa). *P. pachyrhizi Elongation factor 1α* (*PpEF1α*) and *Ubiquitin 5* (*PpUBQ5*) were used to normalize *P. pachyrhizi* gene expression. Soybean *Actin 4* (*GmAct4*) was used as an internal control to normalize soybean *GmPR1* gene expression.

Contact angle measurement on soybean leaves

The surface hydrophobicity on the CNF-treated leaves was investigated based on contact angle measurement using an automatic contact angle meter DM-31(Kyowa Interface Science, Niiza, Japan). The contact angle was measured by dropping 2 µl of water from a syringe attached to the DM-31 automatic contact angle meter. The contact

171 angle was measured on the adaxial and abaxial leaf surfaces with or without 0.1% CNF
172 treatments. The contact angle was analyzed using the multi-functional integrated
173 analysis software FAMAS (Kyowa Interface Science).
174
175 **Results**
176 **Covering soybean leaves with CNF confers resistance against *P. pachyrhizi***
177 To investigate the potential application of CNF in agriculture, especially disease
178 resistance against pathogens, we first treated soybean leaves with two CNF types
179 derived from bamboo (BC) and needle-leaved tree (NC). At 4 hours after spraying with
180 0.1% CNF, we challenged soybean leaves with *P. pachyrhizi* and observed lesion
181 formation including uredinia at 10 days after inoculation. Both CNF-treated leaves
182 showed reduced lesion area compared to control leaves (Fig. 1A). Both CNF-treated
183 leaves showed significantly reduced lesion number compared to control leaves (Fig. 1B).
184 These results indicate that covering soybean leaves with CNF confers resistance against
185 *P. pachyrhizi*.
186 Nanofibers such as chitin nanofibers induce plant immune responses by
187 activating defense-related gene expression (23). Therefore, one could argue that the
188 CNF-induced resistance phenotype in soybean plants may result from defense response
189 activation rather than from the direct effects of CNF treatments against *P. pachyrhizi*. To
190 rule out this possibility, we investigated the expression profiles of the defense marker
191 gene *GmPR1* after CNF treatments. *GmPR1* expression in CNF-treated leaves showed
192 no significant induction compared to control leaves (Fig. S1). These results confirmed
193 that the CNF-induced resistance phenotype against *P. pachyrhizi* is a direct effect of
194 CNF treatment.
195

196 **Covering soybean leaves with CNF suppresses formation of *P. pachyrhizi***
197 **pre-infection structures**

198 Since both CNF-treatments suppressed the lesion number, we next investigated
199 the formation of pre-infection structures including germ-tubes and appressoria on
200 CNF-treated leaves. In control leaves, around 60% of urediniospores germinated, and
201 ~15% and ~30% formed appressoria on adaxial and abaxial leaves, respectively (Fig.
202 2A and Fig. 2B). In CNF-treated leaves, around 60% of urediniospores germinated, and
203 interestingly less than 5% of them formed appressoria on both adaxial and abaxial
204 leaves (Fig. 2A and Fig. 2B). These results suggest that covering soybean leaves with
205 CNF suppresses formation of pre-infection structures including germ-tubes and
206 appressoria.

207

208 **Covering soybean leaves with CNF changes gene expression profiles related to**
209 **formation of pre-infection structures**

210 Ishiga et al. (17) reported that gene expression related to formation of
211 pre-infection structures was induced on the hydrophobic surface based on *P. pachyrhizi*
212 transcriptome analysis. Since CNF-treatments suppressed formation of pre-infection
213 structures including germ-tubes and appressoria, we next investigated gene expression
214 profiles related to formation of pre-infection structures. The expression of *chitin*
215 *synthase 5-1* (*CHS5-1*) and *TKL family protein kinase* was suppressed in CNF-treated
216 leaves at 48 hours after inoculation with *P. pachyrhizi* (Fig. 3A and Fig. 3B).
217 Furthermore, the expression of *metacaspase* and *NADH dehydrogenase* was suppressed
218 in CNF-treated leaves at 24 and 48 hours after inoculation with *P. pachyrhizi* (Fig. 3C
219 and Fig. 3D). These results suggest that covering soybean leaves with CNF changes
220 gene expression profiles related to formation of pre-infection structures.

Chitin synthases (CHSs) are key enzymes in the biosynthesis of the fungal cell wall structural component, chitin. Since *CHS5-1* expression was suppressed in CNF-treated leaves, we next tested the expression profiles of other *P. pachyrhizi CHS* genes in CNF-treated leaves. Except *CHS2-1*, all *CHS* genes transcripts were not significantly suppressed in CNF-treated leaves (Fig. S2B, Fig. S2C, Fig. S2D, Fig. S2E, Fig. 2F, Fig. 2H and Fig. S2H). In addition to *CHS5-1*, *CHS2-1* expression was suppressed in CNF-treated leaves (Fig. S2A). Together, these results suggest that CNF-treatments suppress the expression of *CHS5-1* and *CHS2-1*, resulting in reduced chitin biosynthesis activity in the *P. pachyrhizi* cell wall.

CNF converts leaf surface properties from hydrophobic to hydrophilic

CNF has amphipathic properties, and thus can convert material surface properties from hydrophobic to hydrophilic, and *vice versa* (21). To confirm whether CNF-treatments can convert soybean leaf surface properties from hydrophobic to hydrophilic, we decided to quantify the differences in surface hydrophobicity by measuring the contact angle at the interface of a liquid (water) drop with the leaf surface. A greater contact angle (>90°) is indicative of poor wetting or hydrophobicity. Interestingly, significant differences in the contact angle were observed between control and CNF-treated adaxial leaf surfaces (Fig. S3A). The adaxial leaf surface of control leaves exhibited an average contact angle of 128°, whereas CNF-treated leaves showed a dramatic decrease in the contact angle (around 90°), which is indicative of a hydrophilic surface (Fig. 4A). Similarly, significant differences in the contact angle were observed between control and CNF-treated abaxial leaf surfaces (Fig. S3B). The abaxial leaf surface of control leaves exhibited an average contact angle of 127°, whereas CNF-treated leaves showed a dramatic decrease in contact angle (around 70°;

Fig. 4B). These results clearly indicate that CNF-treatments can convert leaf surface properties from hydrophobic to hydrophilic.

Discussion

We investigated the potential application of CNF in agriculture, especially disease protection in soybean plants against the rust pathogen, *P. pachyrhizi*, and found that CNF-treated soybean leaves conferred resistance against *P. pachyrhizi* (Fig. 1A and Fig. 1B). CNF-treatments can convert the soybean leaf surface properties from hydrophobic to hydrophilic (Fig. 4A and Fig. 4B), resulting in suppression of *P. pachyrhizi* genes involved in the formation of pre-infection structures, including germ-tubes and appressoria (Fig. 3) associated with reduced appressoria formation (Fig. 2). These results provide new insights into CNF application on *P. pachyrhizi* disease management strategies.

We demonstrated that CNF-treatments conferred soybean resistance against *P. pachyrhizi* associated with reduced lesion formation (Fig. 1A and Fig. 1B). The application of chitin nanofibers for plant protection against pathogens has been investigated. Egusa et al. (23) reported that chitin nanofibers effectively reduced fungal and bacterial pathogen infections in *Arabidopsis thaliana* by activating plant defense responses, including reactive oxygen species (ROS) production and defense-related gene expression. Furthermore, chitin nanofiber treatment can reduce the occurrence of Fusarium wilt disease in tomato plants (24). These results suggest that chitin nanofibers activate plant immunity, resulting in reduced pathogen infection. However, we showed no elicitor activity of CNF based on the *GmPR1* defense maker gene expression profiles (Fig. S1). Although there is no similarity to the mechanism by which nanofibers, including cellulose and chitin, function to protect plants against pathogens, both

nanofibers will be able to provide eco-friendly disease control strategies in sustainable agriculture.

Formation of pre-infection structures including germ-tubes and appressoria was significantly suppressed in CNF-treated leaves compared to control leaves (Fig. 2). Consistent with our results, Uppalapati et al. (16) reported the reduced formation of pre-infection structures on a *M. truncatula irg1* mutant, in which the epicuticular waxes were completely defective and the surface property was changed to hydrophilic. These results indicate that properties such as hydrophobicity are important to form *P. pachyrhizi* pre-infection structures during early infection stages. The importance of hydrophobicity and/or epicuticular waxes on the formation of germ-tubes and appressoria has also been reported for other fungal pathogens (25–27). Further characterization of the mechanisms by which fungal pathogens recognize plant surface properties and initiate infection behavior will be needed to develop effective and sustainable disease control methods.

CNF-treatments suppressed gene expression related to chitin formation, including *CHS2* and *CHS5*, which are associated with reduced formation of pre-infection structures (Fig. S2, Fig. 2 and Fig. 3). CHS5 is important in cell wall formation in most filamentous fungi (28, 29). Treitschke et al. (30) reported that an *Ustilago maydis CHS5* mutant Δ*msc1* showed reduced virulence associated with abnormal hyphal morphology. Madrid et al. (31) also demonstrated that CHS5 in *Fusarium oxysporum*, a causal agent of tomato vascular wilt, has a crucial role in virulence and mediates the tomato protective response. A *F. oxysporum CHS5* mutant could not infect tomato, exhibiting abnormal morphologies such as hyphal swelling, due to changes in the cell wall properties (31). These results suggest that *CHS5* gene deficiency or mutation causes morphological abnormalities in fungal cell wall formation, leading to virulence

296 suppression. Together, it is tempting to speculate that suppression of *P. pachyrhizi CHS5*
297 in CNF-treated leaves may result in changes in cell wall properties of *P. pachyrhizi*
298 pre-infection structures. Further characterization of CHS5 based on dsRNA-mediated
299 silencing such as spray-induced gene silencing (SIGS) and host-induced gene silencing
300 (HIGS), in conjunction with analysis of *P. pachyrhizi* cell wall properties on
301 CNF-treated leaves, will be necessary to understand CHS5 molecular function during
302 formation of pre-infection structures.

303 We demonstrated that CNF-treatments suppressed ASR, one of the most
304 important soybean diseases (Fig. 1A and Fig. 1B) associated with reduced formation of
305 pre-infection structures (Fig. 2A and Fig. 2B). Because numerous rust and filamentous
306 fungal pathogens form pre-infection structures during early infection stages, these
307 results imply that CNF might be an additional disease management tool to prevent crop
308 diseases against these pathogens. However, we tested the ability of CNF to protect
309 plants against an obligate biotrophic pathogen, but not other pathogen types, including
310 hemibiotrophs and necrotrophs. Therefore, further characterization of CNF effects on
311 disease suppression not only against fungal pathogens, but also against bacterial
312 pathogens will be needed.

313 In summary, CNF-treatments confer resistance against *P. pachyrhizi*, a causal
314 agent of ASR. Moreover, CNF-treatments can change leaf surface hydrophobicity,
315 resulting in gene suppression related to chitin synthase, which is associated with
316 reduced formation of pre-infection structures including *P. pachyrhizi* germ-tubes and
317 appressoria (Fig. 5). Since CNF is an abundant and renewable biomass in nature, CNF
318 application for plant protection will provide a new avenue into eco-friendly and
319 sustainable disease management.

320

Figure legends

Figure 1. *P. pachyrhizi* lesion formation on CNF-treated soybean leaves

(A) Lesions resulting from *P. pachyrhizi* infection on the abaxial leaf surface of control, leaves covered with 0.1% cellulose nanofiber derived from bamboo (BC) and needle-leaved tree (NC). Soybean plants were spray-inoculated with *P. pachyrhizi* (1 x 10^5 spores/ml), and photographs were taken at 10 days after inoculation. Bars indicate 0.2 cm. (**B)** Lesion numbers resulting from *P. pachyrhizi* infection on the abaxial leaf surface of control, leaves covered with 0.1% cellulose nanofiber derived from bamboo (BC) and needle-leaved tree (NC). Soybean plants were spray-inoculated with *P. pachyrhizi* (1 x 10^5 spores/ml) and lesion numbers were counted to calculate lesion number per cm^2. Vertical bars indicate the standard error of the means (n = 54). Asterisks indicate a significant difference between control and CNF-treatments in a *t* test (** $p < 0.01$).

Figure 2. Suppression of *P. pachyrhizi* pre-infection structures on CNF-treated soybean leaves

P. pachyrhizi pre-infection structure formation on the adaxial (**A**) and abaxial (**B**) surfaces of control, leaves covered with 0.1% cellulose nanofiber derived from bamboo (BC) and needle-leaved tree (NC). Soybean plants were spray-inoculated with *P. pachyrhizi* (2 x 10^5 spores/ml). Photographs were taken at 3 days after inoculation and the percentage of germinated (Ge) urediniospores and differentiated germ-tubes with appressoria (Ap) were evaluated as described in the Methods. Vertical bars indicate the standard error of the means (n = 9). Asterisks indicate a significant difference between control and CNF-treatments in a *t* test (* $p < 0.05$, ** $p < 0.01$).

Figure 3. Gene expression profiles related to formation of *P. pachyrhizi* pre-infection structures on CNF-treated soybean leaves

Gene expression profiles related to *P. pachyrhizi* pre-infection structures including *CHS5-1* (**A**), *TKL family protein kinase* (**B**), *metacaspase* (**C**), and *NADH dehydrogenase* (**D**) during *P. pachyrhizi* early infection steps in control leaves, leaves covered with 0.1% cellulose nanofiber derived from bamboo (BC) and needle-leaved tree (NC). Soybean plants were drop-inoculated with *P. pachyrhizi* (10 µl of 2 x 10^5 spores/ml). Total RNAs including soybean plants and *P. pachyrhizi* were purified at 24 and 48 hours after inoculation, and expression profiles were evaluated using RT-qPCR. *P. pachyrhizi Elongation factor* and *Ubiquitin 5* were used to normalize the samples. Vertical bars indicate the standard error of the means (n = 4). Asterisks indicate a significant difference between control and CNF-treatments in a t test (* $p < 0.05$, ** $p < 0.01$).

Figure 4. Reduction of contact angle and hydrophobicity on CNF-treated soybean leaves

Contact angles of water droplets on the adaxial (**A**) and abaxial (**B**) leaf surface of control, leaves covered with 0.1% cellulose nanofiber derived from bamboo (BC) and needle-leaved tree (NC). Contact angles were evaluated as described in the Methods. Vertical bars indicate the standard error of the means (n = 60). Asterisks indicate a significant difference between control and CNF-treatments in a t test (* $p < 0.05$, ** $p < 0.01$).

Figure 5. Proposed mechanism model by which CNF-treatments confer resistance against *P. pachyrhizi*

CNF-treatments convert leaf surface properties from hydrophobic to hydrophilic. The formation of pre-infection structures, and the associated gene expressions related to these formations are suppressed on CNF-treated leaves, resulting in reduced *P. pachyrhizi* infection. Gt, Ap, and Ht show germ-tubes, appressoria, and haustoria, respectively.

Supplementary Figure S1. Expression of soybean defense marker gene *GmPR1* in response to CNF

Soybean plants were treated with 0.1% cellulose nanofiber derived from bamboo (BC) and needle-leaved tree (NC). Total RNA was purified at 24 hours after treatment and expression profiles were evaluated using RT-qPCR. Soybean *Actin4* (*GmAct4*) was used as an internal control to normalize gene expression. NS indicates not significant between control and CNF-treatments in a *t* test.

Supplementary Figure S2. Expression profiles of *chitin synthases* (*CHSs*), including *CHS2-1* (A), *CHS2-2* (B), *CHS2-3* (C), *CHS3-1* (D), *CHS3-2* (E), *CHS3-3* (F), *CHS4* (G), and *CHS5-2* (H) during the early *P. pachyrhizi* infection stage on the surface of control, leaves covered with 0.1% cellulose nanofiber derived from bamboo (BC) and needle leaf tree (NC)

Soybean plants were drop-inoculated with *P. pachyrhizi* (2×10^5 spores/ml). Total RNAs including soybean plants and *P. pachyrhizi* were purified at 24 and 48 hours after inoculation and expression profiles were evaluated using RT-qPCR. *Elongation factor* and *Ubiquitin 5* were used to normalize the samples. Vertical bars indicate the standard error of the means ($n = 4$). Asterisks indicate a significant difference between control and CNF-treatments in a *t* test (* $p < 0.05$, ** $p < 0.01$).

Supplementary Figure S3. Reduction of contact angle and hydrophobicity on CNF-treated soybean leaves

Contact angles of water droplets on the adaxial (**A**) and abaxial (**B**) leaf surface of control, leaves covered with 0.1% cellulose nanofiber derived from bamboo (BC) and needle-leaved tree (NC). Contact angles were evaluated as described in the Methods.

References

1. Yorinori, J.T., Paiva, W.M., Frederick, R.D., Costamilan, L.M., Bertagnolli, P.F., Hartman, G.E., Godoy, C.V., and Nunes, J. Epidemics of soybean rust (*Phakopsora pachyrhizi*) in Brazil and Paraguay from 2001 to 2003. Plant Disease. 2005; 89: 675–677.
2. Slaminko, T.L., Miles, M.R., Frederick, R.D., Bonde, M.R., and Hartman, G.L. New legume hosts of *Phakopsora pachyrhizi* based on greenhouse evaluations. Plant Disease. 2008; 92: 767–771.
3. Bolton, M.D., Kolmer, J.A., and Garvin, D.F. Wheat leaf rust caused by *Puccinia triticina*. Molecular Plant Pathology. 2008; 9: 563–575.
4. Goellner, K., Loehrer, M., Langenbach, C., Conrath, U., Koch, E., and Schaffrath, U. *Phakopsora pachyrhizi*, the causal agent of Asian soybean rust. Molecular Plant Pathology. 2010; 11: 169–177.
5. Maltby, L., Brock, T.C., and Van den Brink, P.J. Fungicide risk assessment for aquatic ecosystems: importance of interspecific variation, toxic mode of action, and exposure regime. Environmental Science and Technology. 2009; 43: 7556–7563.
6. Godoy, C.V., Bueno, A.d.F., and Gazziero, D.L.P. Brazilian soybean pest management and threats to its sustainability. Outlooks on Pest management. 2015;

421 7. Langenbach, C., Campe, R., Beyer, S.F., Mueller, A.N., and Conrath, U. Fighting
422 Asian soybean rust. Frontiers in Plant Science. 2016; 7: 797.
423 8. Klosowski, A.C., Castellar, C., Stammler, G., and May De Mio, L.L. Fungicide
424 sensitivity and monocyclic parameters related to the *Phakopsora*
425 *pachyrhizi*–soybean pathosystem from organic and conventional soybean
426 production systems. Plant Pathology. 2018; 67: 1697–1705.
427 9. Bromfield, K.R., and Hartwig, E.E. Resistance to soybean rust and mode of
428 inheritance. Crop Science. 1980; 20: 254-255.
429 10. McLean, R., and Byth, D. Inheritance of resistance to rust (*Phakopsora pachyrhizi*)
430 in soybeans. Australian Journal of Agricultural Research. 1980; 31: 951–956.
431 11. Hartwig, E.E. Identification of a fourth major gene conferring resistance to soybean
432 rust. Crop Science. 1986; 26: 1135–1136.
433 12. Garcia, A., Calvo, E.S., de Souza Kiihl, R.A., Harada, A., Hiromoto, D.M., and
434 Vieira, L.G. Molecular mapping of soybean rust (*Phakopsora pachyrhizi*) resistance
435 genes: discovery of a novel locus and alleles. Theor Appl Genet. 2008; 117:
436 545–553.
437 13. Li, S., Smith, J.R., Ray, J.D., and Frederick, R.D. Identification of a new soybean
438 rust resistance gene in PI 567102B. Theoretical and Applied Genetics. 2012; 125:
439 133–142.
440 14. Monteros, M.J., Missaoui, A.M., Phillips, D.V., Walker, D.R., and Boerma, H.R.
441 Mapping and confirmation of the 'Hyuuga' red-brown lesion resistance gene for
442 Asian soybean rust. Crop Science. 2007; 47: 829–834.
443 15. Kawashima, C.G., Guimarães, G.A., Nogueira, S.R., MacLean, D., Cook, D.R.,
444 Steuernagel, B., Baek, J., Bouyioukos, C., Melo, B.o.V., Tristão, G., de Oliveira,
445 J.C., Rauscher, G., Mittal, S., Panichelli, L., Bacot, K., Johnson, E., Iyer, G., Tabor,

446 G., Wulff, B.B., Ward, E., Rairdan, G.J., Broglie, K.E., Wu, G., van Esse, H.P.,
447 Jones, J.D., and Brommonschenkel, S.H. A pigeonpea gene confers resistance to
448 Asian soybean rust in soybean. Nature Biotechnology. 2016; 34: 661–665.
449 16. Uppalapati, S.R., Ishiga, Y., Doraiswamy, V., Bedair, M., Mittal, S., Chen, J.,
450 Nakashima, J., Tang, Y., Tadege, M., Ratet, P., Chen, R., Schultheiss, H., and
451 Mysore, K.S. Loss of abaxial leaf epicuticular wax in *Medicago truncatula*
452 *irg1*/*palm1* mutants results in reduced spore differentiation of anthracnose and
453 nonhost rust pathogens. Plant Cell. 2012; 24: 353–370.
454 17. Ishiga, Y., Upplapapti, S., and Mysore, K.S. Expression analysis reveals a role for
455 hydrophobic or epicuticular wax signals in pre-penetration structure formation of
456 *Phakopsora pachyrhizi*. Plant Signaling and Behavior. 2013; 8: e26959.
457 18. Mondal, S. Preparation, properties and applications of nanocellulosic materials.
458 Carbohydrate Polymers. 2017; 163: 301–316.
459 19. Abe, K., Iwamoto, S., and Yano, H. Obtaining cellulose nanofibers with a uniform
460 width of 15 nm from wood. Biomacromolecules. 2007; 8: 3276–3278.
461 20. Kondo, T., Kose, R., Naito, H., and Kasai, W. Aqueous counter collision using
462 paired water jets as a novel means of preparing bio-nanofibers. Carbohydrate
463 Polymers. 2014; 112: 284–290.
464 21. Kose, R., Kasai, W., and Kondo, T. Switching surface properties of substrates by
465 coating with a cellulose nanofiber having a high adsorbability. Journal of Fiber
466 Science and Technology. 2011; 67: 163–168.
467 22. Yamaoka, Y., Yamanaka, N., and Akamatsu, H. Pathogenic races of soybean rust
468 *Phakopsora pachyrhizi* collected in Tsukuba and vicinity in Ibaraki, Japanese
469 Journal of General Plant Pathology. 2014; 80: 184–188.
470 23. Egusa, M., Matsui, H., Urakami, T., Okuda, S., Ifuku, S., Nakagami, H., and

471 Kaminaka, H. Chitin nanofiber elucidates the elicitor activity of polymeric chitin in
472 plants. Front Plant Sci. 2015; 6: 1098.
473 24. Egusa, M., Parada, R., Aklog, Y.F., Ifuku, S., and Kaminaka, H. Nanofibrillation
474 enhances the protective effect of crab shells against Fusarium wilt disease in tomato.
475 Int J Biol Macromol. 2019; 128: 22–27.
476 25. Mendoza-Mendoza, A., Berndt, P., Djamei, A., Weise, C., Linne, U., Marahiel, M.,
477 Vranes, M., Kämper, J., and Kahmann, R. Physical-chemical plant-derived signals
478 induce differentiation in *Ustilago maydis*. Molecualr Microbiology, 2009; 71:
479 895–911.
480 26. Hansjakob, A., Bischof, S., Bringmann, G., Riederer, M., and Hildebrandt, U.
481 (2010). Very-long-chain aldehydes promote *in vitro* prepenetration processes of
482 *Blumeria graminis* in a dose- and chain length-dependent manner. New Phytol
483 2010; 188: 1039–1054.
484 27. Weidenbach, D., Jansen, M., Franke, R.B., Hensel, G., Weissgerber, W., Ulferts, S.,
485 Jansen, I., Schreiber, L., Korzun, V., Pontzen, R., Kumlehn, J., Pillen, K., and
486 Schaffrath, U. Evolutionary conserved function of barley and Arabidopsis
487 3-KETOACYL-CoA SYNTHASES in providing wax signals for germination of
488 powdery mildew fungi. Plant Physiology. 2014; 166: 1621–1633.
489 28. Takeshita, N., Ohta, A., and Horiuchi, H. CsmA, a class V chitin synthase with a
490 myosin motor-like domain, is localized through direct interaction with the actin
491 cytoskeleton in *Aspergillus nidulans*. Molecular Biology of the Cell. 2005; 16:
492 1961-1970.
493 29. Lenardon, M.D., Munro, C.A., and Gow, N.A. Chitin synthesis and fungal
494 pathogenesis. Current Opinion in Microbiology. 2010; 13: 416–423.
495 30. Treitschke, S., Doehlemann, G., Schuster, M., and Steinberg, G. The myosin motor

domain of fungal chitin synthase V is dispensable for vesicle motility but required for virulence of the maize pathogen *Ustilago maydis*. Plant Cell. 2010; 22: 2476–2494.

31. Madrid, M.P., Di Pietro, A., and Roncero, M.I. Class V chitin synthase determines pathogenesis in the vascular wilt fungus *Fusarium oxysporum* and mediates resistance to plant defence compounds. Molecular Microbiology. 2003; 47: 257–266.
32. Zhao, Y., Chang, X., Qi, D., Dong, L., Wang, G., Fan, S., Jiang, L., Cheng, Q., Chen, X., Han, D., Xu, P., and Zhang, S. (2017). A novel soybean ERF transcription factor, *GmERF113*, increases resistance to *Phytophthora sojae* infection in soybean. Frontiers in Plant Science. 2017; 8: 299.

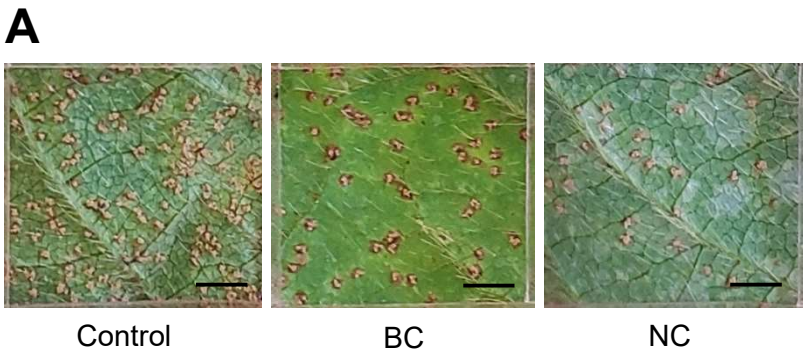

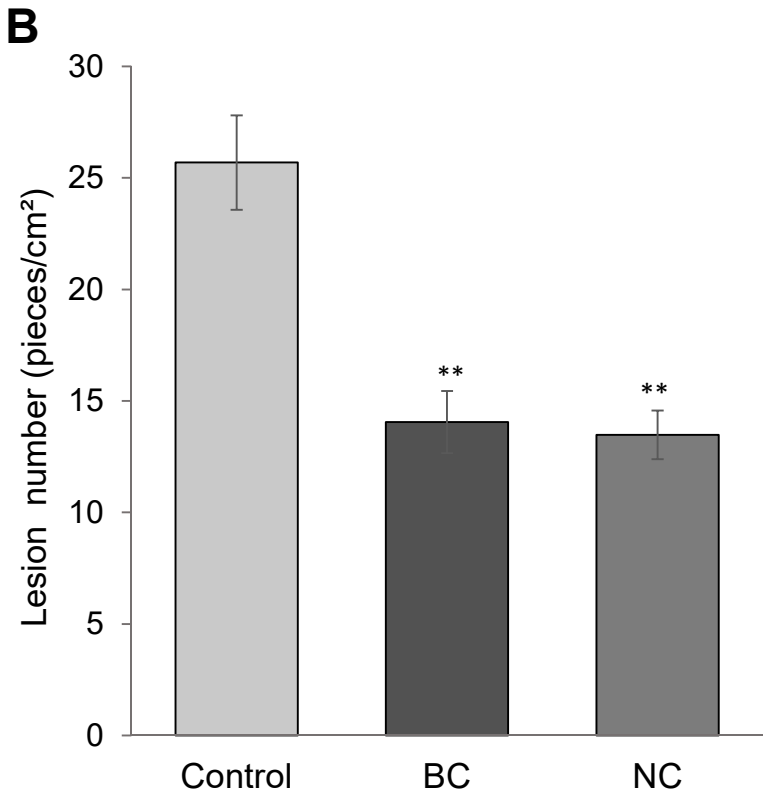

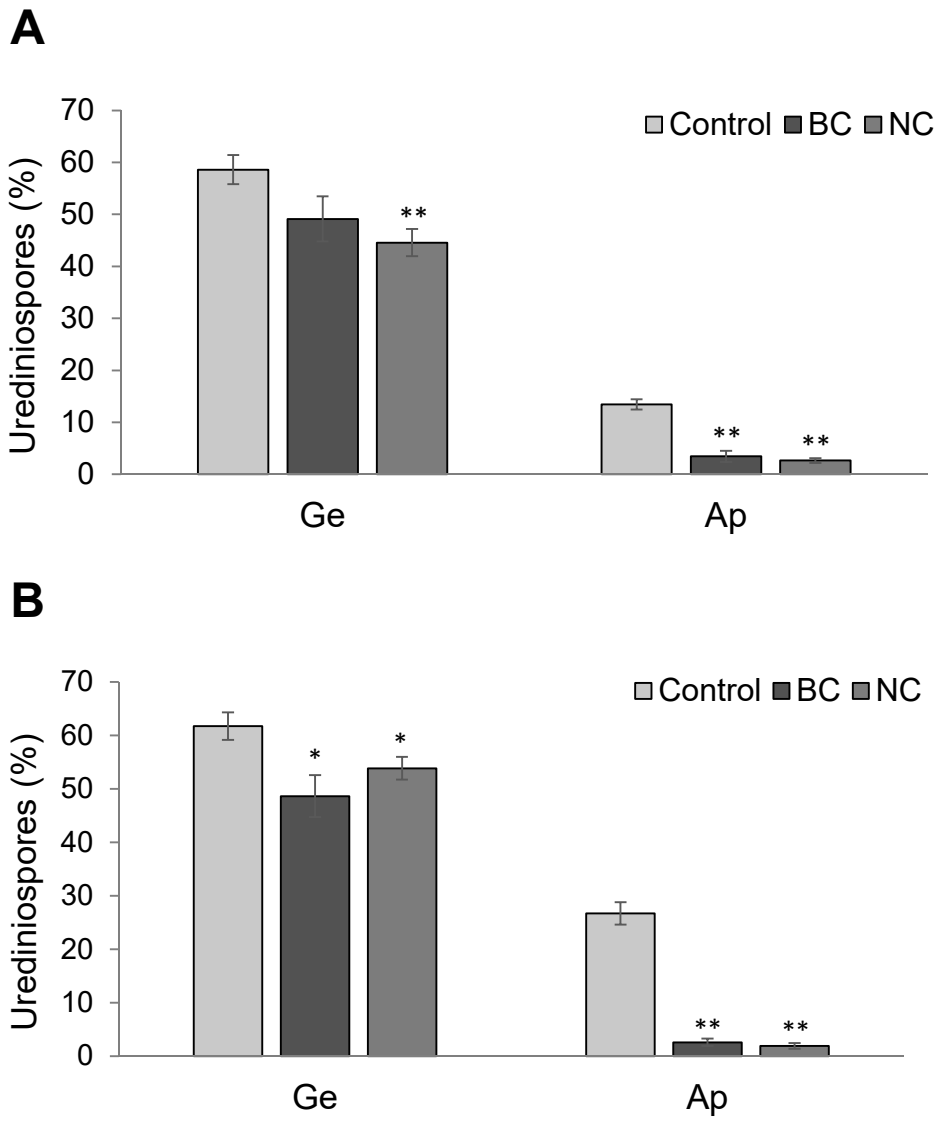

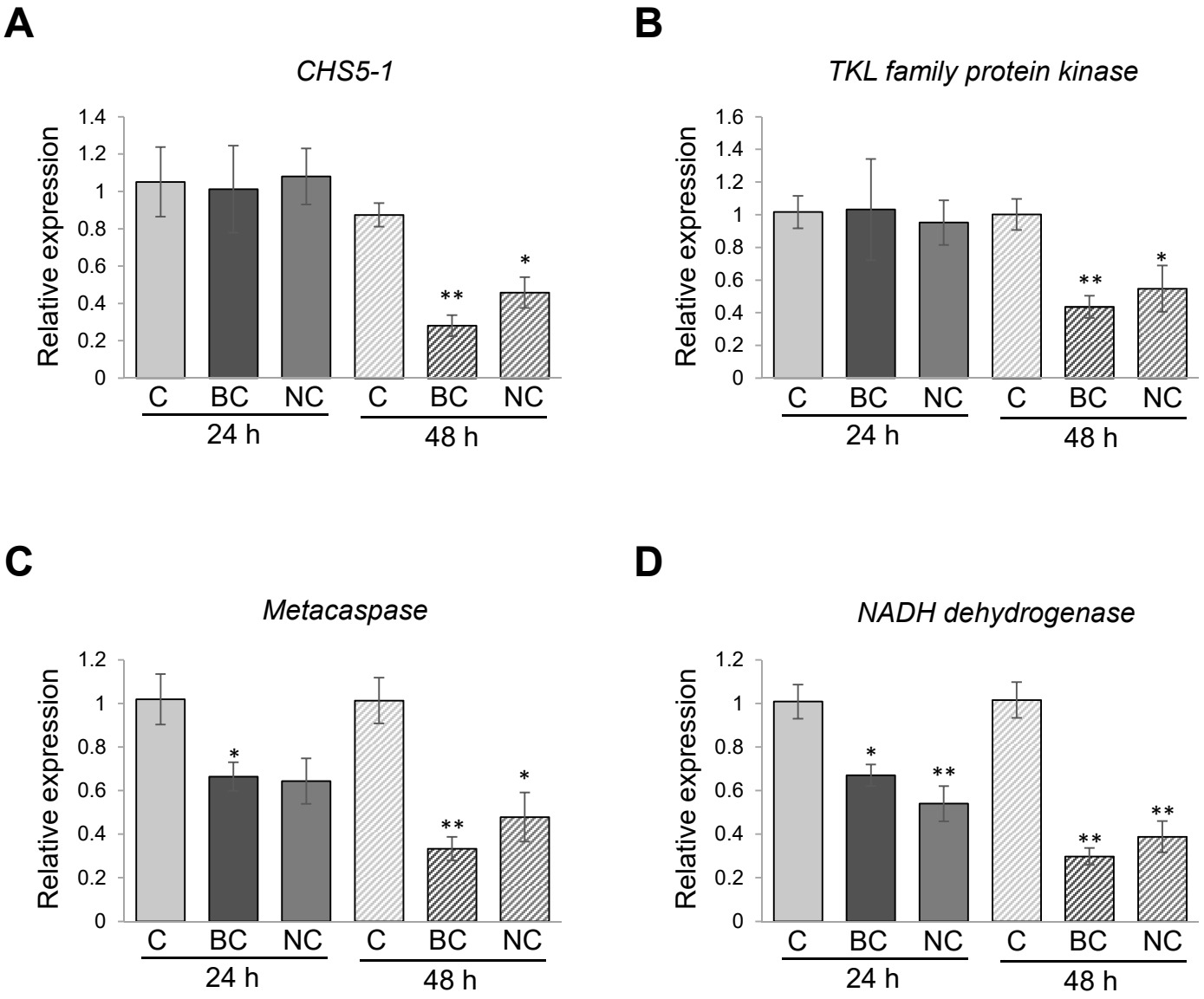

Figure 4

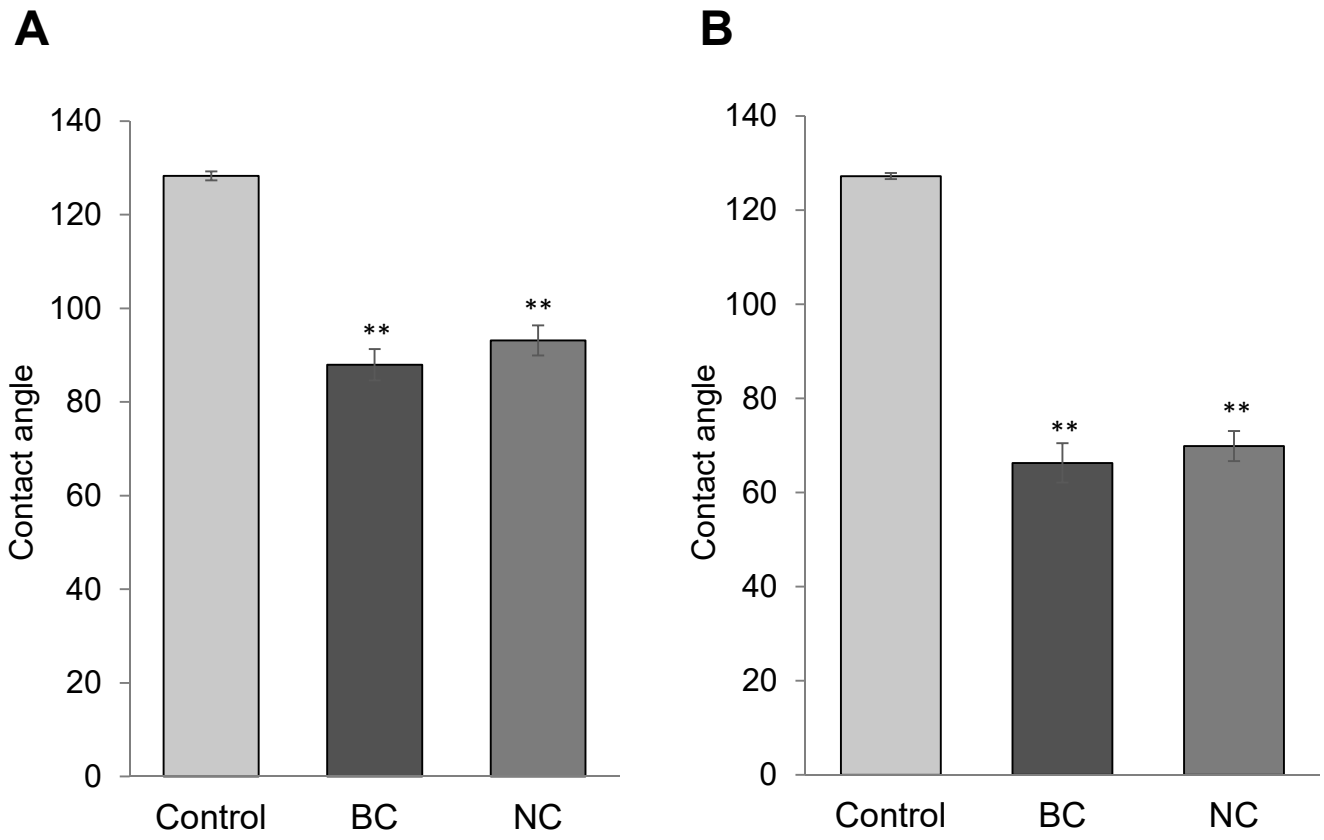

Figure 5